EP-2000-8019

The construction of projection vectors for a Deflated ICCG method applied to problems with extreme contrasts in the coefficients

by

C. Vuik, A. Segal, J.A. Meijerink & G.T. Wijma

Sponsor: EPT-AE-PSA, SEPTAR, Rijswijk

Reviewed by: M.R. Giles, E. Dufour

Approved by: M.R. Giles, E. Dufour

Period of work: Jan 1999 - Dec 1999

ECCN No: Not applicable

Accountcode: 14.32.100E0

SHELL TECHNOLOGY EXPLORATION AND PRODUCTION, RIJSWIJK

Further copies can be obtained from the STEP Library.

The construction of projection vectors for a Deflated ICCG method applied to problems with extreme contrasts in the coefficients

C. Vuik* A. Segal* J.A. Meijerink† G.T. Wijma*

March 17, 2000

Abstract

To predict the presence of oil and natural gas in a reservoir it is important to know the fluid pressure in the rock formations. A mathematical model for the prediction of the fluid pressure history is given by a time-dependent diffusion equation. Application of the finite element method leads to systems of linear equations. A complication is that the underground consists of layers with very large contrasts in permeability. This implies that the symmetric and positive definite coefficient matrix has a very large condition number. Bad convergence behavior of the ICCG method has been observed, and a classical termination criterion is not valid in this problem. In this paper it is proven that the number of small eigenvalues of the IC preconditioned matrix is equal to the number of high-permeability domains, which are not connected to a Dirichlet boundary. To annihilate the bad effect of these small eigenvalues on the convergence, the Deflated ICCG method is used. An efficient method is given to construct the deflation subspace, which subsequently is proven to be a good approximation of the span of the 'small' eigenvectors. As a result of this, the convergence of DICCG is independent of the contrasts in the permeabilities. A theoretical investigation and numerical experiments show that the DICCG method is not sensitive to small perturbations of the deflation vectors. The efficiency of the DICCG method is illustrated by numerical experiments.

Keywords: deflation, IC preconditioned Conjugate Gradients, Poisson equation, porous media, discontinuous coefficients across layers, sensitivity analysis

AMS Subject Classification: 65F10, 65F15, 76S05

1 Introduction

Knowledge of the fluid pressure history in the subsurface is important for an oil company to predict the presence of oil and natural gas in reservoirs and a key factor in safety and environmental aspects of drilling a well. A mathematical model for the prediction of fluid pressures in a geological time scale is based on conservation of mass and Darcy's law ([1] and [6]). The resulting time-dependent three-dimensional non-linear diffusion equation is linearized and integrated in time by the Euler backward method. For the space discretization the finite element method is applied. As a consequence in each time-step a large, sparse linear system of equations has to be solved.

*Delft University of Technology, Faculty of Information Technology and Systems, Department of Applied Mathematical Analysis, Mekelweg 4, 2628 CD Delft, The Netherlands, **e-mail: c.vuik@math.tudelft.nl**

†Shell International Exploration and Production, P.O. Box 60, 2280 AB Rijswijk, The Netherlands

We simplify the problem considerably, taking into account that its characteristic properties are kept. Assume that we have to solve the stationary linear diffusion equation:

$$-\mathrm{div}(\sigma \nabla p) = 0 \text{ on } \Omega, \tag{1}$$

with boundary conditions

$$p = f \text{ on } \partial\Omega^D \text{ (Dirichlet) and } \frac{\partial p}{\partial n} = g \text{ on } \partial\Omega^N \text{ (Neumann)},$$

where $\partial\Omega = \partial\Omega^D \cup \partial\Omega^N$. The fluid pressure and permeability are denoted by p and σ respectively. The domain Ω consists of a number of subdomains in which σ is constant. Two values for σ are considered: $\sigma^h = 1$ for high-permeability subdomains and $\sigma^l = \varepsilon$ for low-permeability subdomains (e.g. the permeabilities ratio for shale and sandstone: ε is of the order 10^{-7} see [16]). The subdomains are denoted by the disjoint sets Ω_i, $i \in \{1, ..., k\}$, which are such that: $\cup_{i=1}^{k} \bar{\Omega}_i = \bar{\Omega}$ and when $\bar{\Omega}_i \cap \bar{\Omega}_j \neq \emptyset$ then $\sigma_i \neq \sigma_j$. Note that in real life applications, the permeability σ is slightly varying in the subdomains. It is straightforward to adapt our method to construct the projection vectors for such a problem.

After a finite element discretization of (1) the linear system

$$Ax = b, \tag{2}$$

with $A \in \mathbb{R}^{n \times n}$ has to be solved. In practical applications we are faced with large regions in a three-dimensional space and as a consequence a large number of finite elements is necessary. The matrix itself is sparse, but due to fill-in a direct method requires too much memory to fit in core. Therefore only iterative methods are acceptable candidates for the solution of the linear systems of equations. Since the coefficient matrix of this system is symmetric and positive definite, a preconditioned Conjugate Gradient method (ICCG) [12] seems to be a suitable iterative method. Unfortunately the earth's crust consists of layers with large contrasts in permeability. Hence a large difference of the extreme eigenvalues is common in the system of equations to be solved. This leads to slow convergence of ICCG and conventional termination criteria [9] are no longer reliable (see [16] for details).

In [8], [16] it has been proven that the number of small eigenvalues of the diagonally scaled matrix is equal to the number (k^s) of high-permeability domains, which boundaries do not contain a part of the Dirichlet boundary. A comparable spectrum has been observed for the IC preconditioned matrix. The bad effect of these eigenvalues on the convergence of ICCG can be annihilated by using the corresponding 'small' eigenvectors as projection vectors in Deflated ICCG [16]. For a literature survey of iterative methods and applications where deflation is used we refer to [16]. The DICCG method has already successfully been used for complicated magnetic field simulations [5]. A related method is recently presented in [14]. Finally in [11, 3] a preconditioner is analyzed for problems which large jumps in the permeabilities arising from reservoir simulation. The preconditioner is the inverse of M, where M is the matrix corresponding to a finite element discretization of (1) with $\sigma \equiv 1$. This preconditioner is only applicable when a fast solution method is available to solve x from $Mx = b$. Another application, where large differences in the coefficients occur, is the fictitious domain method applied to metal casting [13].

To define the Deflated ICCG method we need a set of projection vectors $v_1, ..., v_m$ that form an independent set. The projection on the space A-perpendicular to $\mathrm{span}\{v_1, ..., v_m\}$ is defined as

$$P = I - VE^{-1}(AV)^T \text{ with } E = (AV)^T V \text{ and } V = [v_1 ... v_m] .$$

The solution vector x can be splitted into two parts $x = (I-P)x + Px$. The first part can be calculated as follows $(I-P)x = VE^{-1}VAx = VE^{-1}V^T b$. For the second part we project the solution x_j obtained from DICCG to Px_j.

The Deflated ICCG algorithm reads (see Reference [16]):

DICCG
$j = 0,\ \hat{r}_0 = P^T r_0,\ p_1 = z_1 = L^{-T}L^{-1}\hat{r}_0;$
while $\|\hat{r}_j\|_2 >$ accuracy **do**
$j = j+1;\ \alpha_j = \frac{(\hat{r}_{j-1}, z_{j-1})}{(p_j, P^T A p_j)};$
$x_j = x_{j-1} + \alpha_j p_j;$
$\hat{r}_j = \hat{r}_{j-1} - \alpha_j P^T A p_j;$
$z_j = L^{-T}L^{-1}\hat{r}_j;\ \beta_j = \frac{(\hat{r}_j, z_j)}{(\hat{r}_{j-1}, z_{j-1})};$
$p_{j+1} = z_j + \beta_j p_j;$
end while

Summary of the paper
In Section 2 it is proven that not only the diagonally scaled matrix has k^s small eigenvalues, but that this is also true for the IC preconditioned matrix. Thereafter an efficient construction of the projection vectors in general configurations is given in Section 3. Furthermore it is proven that the span of these vectors is a good approximation of the 'small' eigenspace. A corollary of this is that the convergence of DICCG does not depend on the permeabilities ratio ε. The sensitivity of the method with respect to perturbations of the projection vectors is investigated in Section 4. Finally in Section 5 some numerical experiments are given.

2 Analysis of the IC preconditioned iteration matrix

First we repeat the definition of the Incomplete Choleski (IC) preconditioner. After that it is shown that the preconditioned matrix is scaling invariant. Thereafter the results of [16] with respect to a diagonal preconditioner are generalized to the IC preconditioner. Finally a remark is given concerning an estimate of the condition of the matrix.

The IC preconditioner is defined as follows [12]:

Definition 2.1
Determine the lower triangular matrix L with the following properties:

- $l_{ij} = 0$, *when* $a_{ij} = 0$,
- $(LL^T)_{ij} = a_{ij}$, *when* $a_{ij} \neq 0$.

Let us define $\hat{A} = D^{-\frac{1}{2}} A D^{-\frac{1}{2}}$ where D is an arbitrary diagonal matrix with positive elements on the diagonal. The IC factor of $\hat{A}$ is denoted by $\hat{L}$. In the next theorem we prove that the preconditioned matrix is scaling invariant.

Theorem 2.1
The matrices $L^{-1}AL^{-T}$ and $\hat{L}^{-1}\hat{A}\hat{L}^{-T}$ are identical.

Proof
The nonzero pattern of L and $\hat{L}$ are the same. Suppose $\hat{L} = D^{-\frac{1}{2}}L$ and check the second statement of Definition 2.1:

$$(\hat{L}\hat{L}^T)_{ij} = (D^{-\frac{1}{2}}LL^TD^{-\frac{1}{2}})_{ij} = \frac{1}{\sqrt{d_{ii}}}(LL^T)_{ij}\frac{1}{\sqrt{d_{jj}}} = \frac{1}{\sqrt{d_{ii}}}a_{ij}\frac{1}{\sqrt{d_{jj}}} = (D^{-\frac{1}{2}}AD^{-\frac{1}{2}})_{ij}.$$

These identities imply that $\hat{L}$ is equal to $D^{-\frac{1}{2}}L$. From this the theorem follows since

$$\hat{L}^{-1}\hat{A}\hat{L}^{-T} = L^{-1}D^{\frac{1}{2}}(D^{-\frac{1}{2}}AD^{-\frac{1}{2}})D^{\frac{1}{2}}L^{-T} = L^{-1}AL^{-T}.$$

⊠

As a consequence of this theorem ICCG has the same convergence behavior for the original system $Ax = b$ and the diagonally scaled system $D^{-\frac{1}{2}}AD^{-\frac{1}{2}}y = b$ with $x = D^{-\frac{1}{2}}y$. Therefore we consider the diagonally scaled matrix $\hat{A} = D^{-\frac{1}{2}}AD^{-\frac{1}{2}}$ with $D = diag(A)$ in the remainder of this section. In [16] it is shown that $\hat{A}$ has k^s small eigenvalues. Below we generalize this result to the Incomplete Choleski preconditioned matrix.

We consider the following characteristic configuration: Ω is a rectangular domain, which consists of $2k^s + 1$ plain layers of equal thickness with a high-permeability layer at the top and alternating low- and high-permeability layers further down (see Figure 1). In order to simplify the proofs that

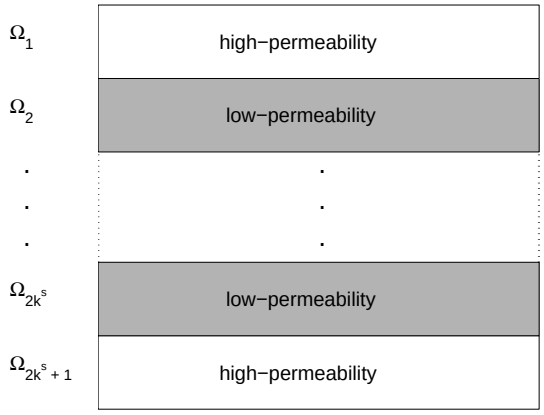

Figure 1: A problem with $2k^s + 1$ plain layers of equal thickness

will be given later on, the unknowns are renumbered in the following way: first all high-permeability unknowns are numbered per layer from top to bottom and next all low-permeability unknowns. Unknowns on the interface of a low- and high-permeability layer will be considered as high-permeability unknowns. Let Δ_h^N, Δ_h^{DT} and Δ_h^D be the Finite Element matrices of the Laplacian on a single layer with respectively homogeneous Neumann boundary conditions on all boundaries, Dirichlet boundary conditions on the top boundary and Dirichlet boundary conditions on top and bottom boundaries. In Δ_h^{DT} and Δ_h^D a homogeneous Neumann boundary condition is posed on all other boundaries.

Theorem 2.2
For ε *small enough the* IC *preconditioned matrix* $\hat{L}^{-1}\hat{A}\hat{L}^{-T}$ *has only* k^s *eigenvalues of* $O(\varepsilon)$.

Proof
Using the Finite Element discretization as given in [16] the matrix $\hat{A}$ can be splitted into an ε dependent and an ε independent part :

$$\hat{A} = \hat{\Delta} + \mathcal{E}, \tag{3}$$

where $\hat{\Delta}$ is the block-diagonal matrix with as first block $\hat{\Delta}_h^{DT}$, the diagonally scaled Δ_h^{DT}, and then further down alternating $\hat{\Delta}_h^D$, the scaled Δ_h^D, and $\hat{\Delta}_h^N$, the scaled Δ_h^N. From [16] it follows that $\|\mathcal{E}\|_2 = \mathrm{O}(\sqrt{\varepsilon})$.

Consider the Incomplete Choleski decomposition $\tilde{L}\tilde{L}^T$ of the matrix $\hat{\Delta}$. Due to its block diagonal structure the Choleski factor is also block diagonal. The existence of the non-singular IC decomposition of $\hat{\Delta}^{DT}$ and $\hat{\Delta}^D$ follows from [12]. Under mild conditions (which are fullfilled in our problem) Kaasschieter ([10] Theorem 3.2) has proven that an IC decomposition exists for the singular matrix $\hat{\Delta}^N$ and the resulting Choleski factor is non-singular. This implies that $\tilde{L}$ exists and $\lambda_{\min}(\tilde{L}\tilde{L}^T) > 0$.

In order to prove $\hat{L}\hat{L}^T = \tilde{L}\tilde{L}^T + \hat{\mathcal{E}}$, with $\|\hat{\mathcal{E}}\|_2 = \mathrm{O}(\sqrt{\varepsilon})$, we first show that

$$\hat{L} = \tilde{L} + \mathrm{O}(\sqrt{\varepsilon}). \tag{4}$$

The elements of $\hat{L}$ are determined by the following formula's:

$$\hat{l}_{ij} = 0, \text{ when } \hat{a}_{ij} = 0, \text{ else } \hat{l}_{ij} = (\hat{a}_{ij} - \sum_{k=1}^{j-1} \hat{l}_{ik}\hat{l}_{jk})/\hat{l}_{jj} \text{ for } j < i\,, \tag{5}$$

$$\hat{l}_{ii} = \sqrt{\hat{a}_{ii} - \sum_{k=1}^{i-1} \hat{l}_{ik}^2}. \tag{6}$$

Equation (4) is proven by induction. The Induction Hypothesis is:

$$\hat{l}_{ij} = \tilde{l}_{ij} + \mathrm{O}(\sqrt{\varepsilon}),\ 1 \le j \le i. \tag{7}$$

The start of the induction is possible because the first block of $\hat{A}$ and $\hat{\Delta}$ are identical.

For $\hat{l}_{i+1,j},\ 1 \le j \le i$ we distinguish two cases:

(i) $\hat{a}_{i+1,j} = \mathrm{O}(1)$
Using (5), (3), and (7) we obtain $\hat{l}_{i+1,j} = \tilde{l}_{i+1,j} + \mathrm{O}(\sqrt{\varepsilon})$.

(ii) $\hat{a}_{i+1,j} = \mathrm{O}(\sqrt{\varepsilon})$
In this case $\tilde{l}_{i+1,j} = 0$ and one has to show that $\hat{l}_{i+1,j} = \mathrm{O}(\sqrt{\varepsilon})$. Due to our ordering of the unknowns $\hat{a}_{i+1,k} = \mathrm{O}(\sqrt{\varepsilon})$ for $k < j$ and thus $\hat{l}_{i+1,k} = \mathrm{O}(\sqrt{\varepsilon})$ for $k < j$. Furthermore $\hat{l}_{jj} = \tilde{l}_{jj} + \mathrm{O}(\sqrt{\varepsilon})$, together with $\tilde{l}_{jj} > 0$ implies that $\hat{l}_{jj} > 0$ for ε small enough. These estimates combined with (5) show that $\hat{l}_{i+1,j} = \mathrm{O}(\sqrt{\varepsilon})$.

For $\hat{l}_{i+1,i+1}$ we obtain from (6), (3), and (7) that

$$\hat{l}_{i+1,i+1} = \sqrt{\hat{\Delta}_{i+1,i+1} - \sum_{k=1}^{i} \tilde{l}_{i+1,k}^2 + \mathrm{O}(\sqrt{\varepsilon})}.$$

Since $\tilde{l}_{i+1,i+1} \neq 0$ it follows that $\hat{l}_{i+1,i+1} = \tilde{l}_{i+1,i+1} + O(\sqrt{\varepsilon})$.

From Equation (4) it easily follows that

$$\hat{L}\hat{L}^T = \tilde{L}\tilde{L}^T + \hat{\mathcal{E}}, \text{ with } \|\hat{\mathcal{E}}\|_2 = O(\sqrt{\varepsilon}).$$

The minimax characterization ([7] Theorem 8.1.5) can be used to derive the inequalities

$$\lambda_{\min}(\hat{L}\hat{L}^T) \geq \lambda_{\min}(\tilde{L}\tilde{L}^T) - O(\sqrt{\varepsilon}) \text{ and } \lambda_{\max}(\hat{L}\hat{L}^T) \leq \lambda_{\max}(\tilde{L}\tilde{L}^T) + O(\sqrt{\varepsilon}).$$

For ε small enough we have the bound $\lambda_{\min}(\hat{L}\hat{L}^T) \geq \frac{1}{2}\lambda_{\min}(\tilde{L}\tilde{L}^T) > 0$, which is independent of ε. The Courant-Fisher Minimax Theorem ([7] Theorem 8.1.2) can be used to show that

$$\frac{1}{\lambda_{\max}(\hat{L}\hat{L}^T)}\lambda_k(\hat{A}) \leq \lambda_k(\hat{L}^{-1}\hat{A}\hat{L}^{-T}) \leq \frac{1}{\lambda_{\min}(\hat{L}\hat{L}^T)}\lambda_k(\hat{A}).$$

So the number and size of small eigenvalues of $\hat{A}$ and $\hat{L}^{-1}\hat{A}\hat{L}^{-T}$ are the same. Using Theorem 3.1 from [16] the theorem is proven. ⊠

This section is concluded with a remark on estimating the condition of $\hat{A}$. When a linear system is solved by an iterative method it is important to have an estimate of the condition number of the matrix. This estimate can be combined with the machine precision to derive a lower bound for the norm of the residual. It has no sense to iterate further when the norm of the residual is below this bound. We know that $\hat{A}$ is bad conditioned, however, we have no test to detect this, since the classical method to estimate the smallest eigenvalue fails [9, 16]. Another method to estimate the condition of a matrix is to estimate the condition of its Choleski factor [4, 2]. Such a method is not usefull in this problem because it follows from the proof of Theorem 2.2 that the incomplete Choleski factor $\hat{L}$ is well conditioned.

3 The construction of the projection vectors

In [16] the 'small' eigenvectors have been computed and analyzed for a simple test problem. This analysis suggests that the eigenvectors are constant in high-permeability layers and satisfy (1) in low-permeability layers with appropriate boundary conditions. The computation of eigenvectors is expensive and therefore an efficient way to construct the projection vectors for layered problems (see Figure 1) is given in [16]. In this construction the vertical cross sections of the projection vectors v_i are made such that:

- the value of v_i is one in the $i+1^{\text{th}}$ high-permeability layer including interface points and zero in the other high-permeability layers,
- the value of v_i in low-permeability layers is a linear interpolation of its values on the interfaces.

Below we give a generalization of the construction of the projection vectors for general geometries. Furthermore a proof is given that the space spanned by these projection vectors is a good approximation of the 'small' eigenspace of the (diagonal or IC) preconditioned matrix. To construct the projection vectors the subdomains are ordered as follows:

Definition 3.1
The high-permeability subdomains are numbered first: $\Omega_i,\ i \in \{1,...,k^h\}$. *Furthermore the first* k^s *high-permeability subdomains are such that* $\bar{\Omega}_i \cap \partial\Omega^D = \emptyset,\ i \in \{1,...,k^s\}$.

In other words the first k^s subdomains are highly permeable and their boundaries do not contain a part of the Dirichlet boundary. This ordering is a generalization of the ordering used in Section 2.

Definition 3.2
The projection vectors v_i for $i \in \{1,...,k^s\}$ are defined as:

- $v_i = 1$ *on* $\bar{\Omega}_i$ *and* $v_i = 0$ *on* $\bar{\Omega}_j, j \neq i, j \in \{1,...,k^h\}$,
- v_i *satisfies the finite element discretization of the equation:*

$$-div(\sigma_j \nabla v_i) = 0 \text{ on } \Omega_j,\ j \in \{k^h+1,...,k\},$$

where Dirichlet boundary conditions are used at the interfaces ($\partial\Omega_j \cap \Omega$) and homogeneous Dirichlet and Neumann boundary conditions are used at outer boundaries ($v_i = 0$ on $\bar{\Omega}_j \cap \partial\Omega^D$ and $\frac{\partial v_i}{\partial n} = 0$ on $\bar{\Omega}_j \cap \partial\Omega^N$).

Note that the projection vectors v_i are independent of ε. In the high-permeability domains the vectors v_i can also be interpreted as a solution of (1) with Dirichlet boundary conditions equal to 1 for $\partial\Omega_i$ and equal to 0 for $\partial\Omega_j, j \neq i, j \in \{1,...,k^h\}$.

We first show that $\|D^{-1}Av_i\|_\infty = O(\varepsilon)$, where $D = \text{diag}(A)$. Thereafter we prove that the vectors v_i are independent, so $\text{span}\{v_1,...,v_{k^s}\}$ approximates the 'small' eigenspace of the diagonally scaled matrix.

Assumption 3.3
We assume that the finite element discretization is consistent, which means that the discretization error is zero for a constant function. The subdomains Ω_i are approximated by polygons and each element is contained in only one polygon. Finally we assume that the off-diagonal elements of A are non-positive.

This last assumption means that the finite element grid must satisfy certain requirements with respect to the angles of the elements. This is a sufficient condition for our proofs, however, the method has a wider range of applicability. Let the vector $\mathbf{x}_m$ contain the space coordinates of grid point m. The j^{th} component of vector v_i is denoted by $(v_i)_j$. A consequence of Assumption 3.3 (consistency) is:

$$\Sigma_{j=1}^{n} a_{mj} = 0 \text{ for } \mathbf{x}_m \in \bar{\Omega} \setminus \partial\Omega^D. \tag{8}$$

For every projection vector v_i we define an index set $\mathbb{I}_i \subset \{1,...,n\}$, which contains the indices of all points on the interfaces of the low-permeability domains which are neighbors of Ω_i.

Theorem 3.1
When Assumption 3.3 is fulfilled the vectors v_i as defined in Definition 3.2 are such that

$$\|D^{-1}Av_i\|_\infty = O(\varepsilon), i \in \{1,...,k^s\}.$$

Proof
We first prove

$$(Av_i)_m = 0 \text{ for } m \in \{1,...,n\} \setminus \mathbb{I}_i. \tag{9}$$

For $\mathbf{x}_m \in \Omega_j \cup (\bar{\Omega}_j \cap \partial\Omega), j \in \{1,...,k^s\}$ component $(v_i)_m$ is equal to the components of v_i in the neighboring points. So (9) follows from equation (8). From Definition 3.2 we see that (9) holds for $\mathbf{x}_m \in \Omega_j \cup (\bar{\Omega}_j \cap \partial\Omega), j \in \{k^s+1,...,k^h\}$. On a low-permeability subdomain ($\mathbf{x}_m \in \Omega_j \cup (\bar{\Omega}_j \cap \partial\Omega), j \in \{k^h+1,...,k\}$) equation (9) also follows from Definition 3.2. Finally when $\mathbf{x}_m$ is on an interface where v_i has zero components on the low-permeability subdomain then all components of v_i are zero in the high-permeability subdomain and thus equation (9) holds. This implies $(D^{-1}Av_i)_m = 0$ for $m \in \{1,...,n\} \setminus \mathbb{I}_i$.

For an $m \in \mathbb{I}_i$ we split its neighbors into two sets $\mathbb{J}_m^h$ and $\mathbb{J}_m^l$. The sets $\mathbb{J}_m^h$, $\mathbb{J}_m^l$ contain the indices of the neighboring points in the high-, low-permeability subdomain respectively. The set $\mathbb{J}_m^h$ also contains the indices of the neighboring points at the interface. This implies:

$$\begin{aligned} a_{mj} &= O(1), \text{ for } j \in \mathbb{J}_m^h, \\ a_{mj} &= O(\varepsilon), \text{ for } j \in \mathbb{J}_m^l. \end{aligned} \tag{10}$$

Assumption 3.3 ($a_{mj} \leq 0, j \neq m$) together with (8), and (10) imply

$$D_{mm} = a_{mm} = -\Sigma_{j \in \mathbb{J}_m^h \cup \mathbb{J}_m^l} a_{mj} = O(1). \tag{11}$$

Equation (8) combined with $(v_i)_j = (v_i)_m$ for $j \in \mathbb{J}_m^h$ yields

$$(Av_i)_m = \Sigma_{j \in \mathbb{J}_m^l} a_{mj}((v_i)_j - (v_i)_m). \tag{12}$$

From the maximum principle we know that $(v_i)_j \in [0,1]$ so $(Av_i)_m = O(\varepsilon)$. Together with $D_{mm} = O(1)$ the result is proven. ⊠

Corollary
For $m \in \mathbb{I}_i$ an $O(1)$ perturbation of $(v_i)_j, j \in \mathbb{J}_m^h$ leads to $\|D^{-1}Av_i\|_\infty = O(1)$, whereas an $O(1)$ perturbation of $(v_i)_j, j \in \mathbb{J}_m^l$ leads to $\|D^{-1}Av_i\|_\infty = O(\varepsilon)$.

This means that a large perturbation of v_i in the low-permeability layer leads to a small perturbation in the matrix vector product $D^{-1}Av_i$.

Definition 3.4
The normalized eigenvectors of $D^{-1}A$ are denoted by u_i:

$$D^{-1}Au_i = \lambda_i u_i, i = 1,...,n;$$

where the eigenvalues are ordered: $\lambda_1 \leq \lambda_2 \leq ... \leq \lambda_n$.

In the following theorem we show that the space spanned by $\{v_1,...,v_{k^s}\}$ is 'nearly' a subspace of the 'small' eigenspace span$\{u_1,...,u_{k^s}\}$. With 'nearly' a subspace we mean that the norm of the component of a vector $v \in \{v_1,...,v_{k^s}\}$ outside the subspace span$\{u_1,...,u_{k^s}\}$ is small.

Theorem 3.2
For $V_{k^s} = [v_1...v_{k^s}]$ and $U_{k^s} = [u_1...u_{k^s}]$ the following expression holds:

$$V_{k^s} = U_{k^s}Z + E, \tag{13}$$

where $\|E\|_2 = O(\sqrt{\varepsilon})$.

Proof
The vector v_1 can be written as a linear combination of the eigenvectors:

$$v_1 = \Sigma_{j=1}^{n} \alpha_j u_j. \tag{14}$$

Theorem 3.1 implies $\|D^{-1}Av_1\|_2^2 \leq O(\varepsilon^2)$. Substitution of (14) gives:

$$\|D^{-1}Av_1\|_2^2 = \|\Sigma_{j=1}^{n} \lambda_j \alpha_j u_j\|_2^2.$$

The eigenvectors $D^{\frac{1}{2}}u_j$ of $D^{-\frac{1}{2}}AD^{-\frac{1}{2}}$ are orthogonal. This property is used in the following derivation:

$$\|D^{-1}Av_1\|_2^2 \geq \lambda_{\min}(D^{-1})\|\Sigma_{j=1}^{n} \lambda_j \alpha_j D^{\frac{1}{2}} u_j\|_2^2$$

$$= \lambda_{\max}(D)\Sigma_{j=1}^{n} \lambda_j^2 \alpha_j^2 \|D^{\frac{1}{2}}u_j\|_2^2 \geq \lambda_{\max}(D)\lambda_{\min}(D)\Sigma_{j=1}^{n} \lambda_j^2 \alpha_j^2.$$

Since $\lambda_{\max}(D) = O(1)$ and $\lambda_{\min}(D) = O(\varepsilon)$ we obtain:

$$\Sigma_{j=1}^{k^s} \lambda_j^2 \alpha_j^2 + \Sigma_{j=k^s+1}^{n} \lambda_j^2 \alpha_j^2 \leq O(\varepsilon).$$

Rearranging the terms shows that

$$\lambda_{k^s+1}^2 \Sigma_{j=k^s+1}^{n} \alpha_j^2 \leq \Sigma_{j=k^s+1}^{n} \lambda_j^2 \alpha_j^2 \leq O(\varepsilon),$$

because $\Sigma_{j=1}^{k^s} \alpha_j^2$ is bounded. Since $\lambda_{k^s+1} = O(1)$ it follows that $\Sigma_{j=k^s+1}^{n} \alpha_j^2 = O(\varepsilon)$. This can be shown for every $v_i, i \in \{1,...,k^s\}$ so the theorem is proven. ⊠

Note that the projection vectors $v_1,...,v_{k^s}$ are linearly independent, because for $\mathbf{x}_m \in \Omega_i$, $i \in \{1,...,k^s\}, (v_i)_m = 1$, and $(v_j)_m = 0$ for $j \neq i$. As a consequence of this the matrix $V_{k^s}^T V_{k^s}$ is non-singular. This can be used to show that the 'small' eigenspace span$\{u_1,...,u_{k^s}\}$ is 'nearly' a subspace of the space spanned by $\{v_1,...,v_{k^s}\}$.

Theorem 3.3
For $V_{k^s} = [v_1...v_{k^s}]$ and $U_{k^s} = [u_1...u_{k^s}]$ the following expression holds:

$$U_{k^s} = V_{k^s} Z^{-1} + \hat{E}, \tag{15}$$

where $\|\hat{E}\|_2 = O(\sqrt{\varepsilon})$.

Proof
From Theorem 3.2 it follows that

$$V_{k^s}^T V_{k^s} = Z^T U_{k^s}^T U_{k^s} Z + \tilde{E} = Z^T Z + \tilde{E},$$

where $\|\tilde{E}\|_2 = O(\sqrt{\varepsilon})$. From the minimax characterization ([7], Theorem 8.1.5) we obtain the bound

$$\lambda_{\min}(Z^T Z) \geq \lambda_{\min}(V_{k^s}^T V_{k^s}) - O(\sqrt{\varepsilon}).$$

Since $V_{k^s}^T V_{k^s}$ is non-singular $\lambda_{\min}(Z^T Z) > 0$ for ε small enough and Z is non-singular. Post-multiplying (13) by Z^{-1} gives:

$$U_{k^s} = V_{k^s} Z^{-1} - E Z^{-1}. \tag{16}$$

The theorem now follows from (15) and (16) because

$$\|\hat{E}\|_2 = \|EZ^{-1}\|_2 \leq (\lambda_{\min}(Z^TZ))^{-\frac{1}{2}}\|E\|_2 = O(\sqrt{\varepsilon}).$$

$\boxtimes$

This theorem motivates the use of the vectors $\{v_1, ..., v_{k^s}\}$ in the Deflated CG method applied to the diagonally scaled matrix to annihilate the effect of the small eigenvalues.

In Section 2 it has been shown that the IC preconditioned matrix has k^s eigenvalues of $O(\varepsilon)$. Below we prove that the vectors $\{v_1, ..., v_{k^s}\}$ can also be used as projection vectors in the DICCG method.

Theorem 3.4
When Assumption 3.3 is fulfilled, the vectors v_i as defined in Definition 3.2 are such that

$$\|L^{-T}L^{-1}Av_i\|_2 = O(\varepsilon), i \in \{1, ..., k^s\}.$$

Proof
The proof of this theorem is based on the results presented in Theorem 3.1. To use these results we note:

$$\|L^{-T}L^{-1}Av_i\|_2 = \|L^{-T}L^{-1}DD^{-1}Av_i\|_2 \leq \lambda_{\max}(L^{-T}L^{-1}D)\|D^{-1}Av_i\|_2.$$

Since $L^{-T}L^{-1}D$ and $\hat{L}^{-T}\hat{L}^{-1}$ are similar, their spectra are identical. From the proof of Theorem 2.2 we have that $\lambda_{\max}(\hat{L}^{-T}\hat{L}^{-1}) = 1/\lambda_{\min}(\hat{L}\hat{L}^T)$ is bounded. This combined with Theorem 3.1 leads to the inequality:

$$\|L^{-T}L^{-1}Av_i\|_2 \leq \lambda_{\max}(\hat{L}^{-T}\hat{L}^{-1})\sqrt{n}\|D^{-1}Av_i\|_\infty = O(\varepsilon).$$

$\boxtimes$

Analogous to Theorem 3.3 one can prove that the 'small' eigenspace of $L^{-T}L^{-1}A$ is 'nearly' a subspace of the span$\{v_1, ..., v_{k^s}\}$. This suggests that the convergence of DICCG is independent of the ratio of the high and low permeability. This is confirmed by numerical experiments in Section 5.1.

We conclude this section with some remarks about an efficient implementation of the DICCG method. It follows from Definition 3.2, that each projection vector v_i is sparse because it is zero everywhere except on $\bar{\Omega}_i$ and its neighboring subdomains. The application of the projection P to a vector consists of inner products and vector updates with v_i and Av_i. The matrix vector product Av_i is less sparse than v_i. The fill-in occurs at the grid points connected to the domain where v_i is non-zero. The number of grid points where Av_i is non-zero is defined as N_i. It is easy to see that the application of P costs approximately $3\sum_{i=1}^{k^s} N_i$ floating point operations. To store v_i and Av_i, $2\sum_{i=1}^{k^s} N_i$ memory positions are necessary. In many applications $\sum_{i=1}^{k^s} N_i$ is less than $2n$. However one can have problems where $N_i \approx n$, which makes DICCG unattractive. An example of this: assume that the domain Ω consists of a low-permeability subdomain which contains k^s subdomains with a high-permeability. Inspection of the computed projection vectors shows that large parts of them are close to zero. Ignoring the small components in the projection vectors, makes DICCG feasible again. In Section 5.2 such a problem is investigated by numerical experiments.

Another important point is the cost to compute the projection vectors on the low-permeability subdomains. The construction implies that a number of diffusion problems have to be solved. The amount of work to solve these sub-problems is small with respect to the total amount of work. The reasons for this are:

- the size of the sub-problems is small,
- the sub-matrices are obtained by copying the relevant part of the original matrix,
- the preconditioned sub-matrices are well conditioned,
- it is sufficient to have an approximation of the sub-solution with a low accuracy.

The final reason is investigated in more detail in the following section.

4 Sensitivity investigation of DICCG

In Section 3 a method is given to construct projection vectors, which span is close to the 'small' eigenspace. An important question is how sensitive is DICCG to perturbations in these approximations. In Section 4.1 we analyze the dependence of DICCG to perturbations of the projection vectors in a simple case. Some numerical experiments to validate our analysis are given in Section 4.2. Finally in Section 4.3 we investigate numerically the occurrence of small eigenvalues when a high-permeability domain is only weakly connected to a Dirichlet boundary.

4.1 Analysis of a perturbed projection vector

We consider a problem where the matrix $A_{IC} = L^{-1}AL^{-T}$ has one small eigenvalue λ_1. The normalized eigenvectors of A_{IC} are denoted by w_i. For simplicity we assume that $\lambda_2 = 1$, and that the perturbed projection vector is given by

$$v_1 = w_1 + \alpha w_2. \tag{17}$$

Since A_{IC} is symmetric the eigenvectors w_i are orthonormal. The perturbed projection operator is

$$P = I - v_1 E^{-1} (A_{IC} v_1)^T,$$

where $E = (A_{IC}v_1)^T v_1 = \lambda_1 + \alpha^2$. Consider the eigenvectors of $P^T A_{IC}$. From the definition of P it follows that $P^T A_{IC} v_1 = 0$. Furthermore (17) implies that $P^T A_{IC} w_i = \lambda_i w_i$, for $i = 3, \ldots, n$. Finally the vector $\alpha w_1 - w_2$ is also an eigenvector of $P^T A_{IC}$ and its eigenvalue is $\lambda_{per} = \frac{\lambda_1(1+\alpha^2)}{\lambda_1+\alpha^2}$. For α small $\lambda_{per} \approx 1 = \lambda_2$. In Table 1 we give λ_{per} for $\lambda_1 = 10^{-9}$ and some values of α. This analysis teaches

α	0	10^{-4}	10^{-3}	10^{-2}	10^{-1}	1
λ_{per}	1	0.0909	10^{-4}	10^{-5}	10^{-7}	$2 \cdot 10^{-9}$

Table 1: Value of λ_{per} for various values of α

us the following: when the projection vectors are perturbed the smallest eigenvalue remains exactly zero, however the smallest but one eigenvalue can change considerably. So if the perturbation of a projection vector is too large deflation with this perturbed vector does not help.

In order to use DICCG we approximate the eigenvectors u_i of $L^{-T}L^{-1}A$. The eigenvectors u_i and w_i are related: $w_i = L^T u_i = \hat{L}^T D^{\frac{1}{2}} u_i$. From Section 2 we know that the elements of $\hat{L}$ are O(1), whereas the elements of $D^{\frac{1}{2}}$ are O(1) in high-permeability domains and $O(\sqrt{\varepsilon})$ in low-permeability domains. So perturbations of u_i in a low-permeability domain lead to small perturbations of w_i and λ_{per}. In the following section we compare the results obtained from this analysis with numerical experiments.

4.2 Validation of the perturbation analysis

As a test problem we consider the straight layer problem as given in [16]. This problem consists of 7 horizontal layers with a sandstone layer ($\sigma = 1$) at the top and alternately shale ($\sigma = 10^{-7}$) and sandstone layers further down.

Two experiments are done. In the first experiment a random vector is added to the projection vector in the shale layers. The amplitude of this vector is $\frac{\alpha}{2}$ and it is zero at the interfaces. The results are given in Table 2. The number of iterations increase for increasing α, however even for $\alpha = 1$ DICCG is much faster than ICCG. We observe that the smallest eigenvalue only changes considerably for $\alpha = 1$. For this choice λ_{per} is of the same order as the square root of the smallest eigenvalue of the original matrix. This agrees well with our analysis. Moreover it appears that the difference between the estimated and exact error is relatively small compared to the case of no deflation.

α	0	10^{-2}	10^{-1}	1	ICCG
λ_{per}	0.164	0.164	0.164	$8.2 \cdot 10^{-3}$	$1.6 \cdot 10^{-9}$
n	14	14	15	24	54

Table 2: Newly introduced small eigenvalue (λ_{per}) and number of iterations (n) needed before DICCG (or ICCG) reaches the required accuracy (perturbation α is restricted to the shale layers)

In the second example we perturb the nonzero parts of the projection vectors v_i also in the sandstone layer Ω_i. In Table 3 the smallest nonzero eigenvalue λ_{per} and the number of iterations are given. Note that qualitatively there is a good correspondence between the results given in Table 1 and Table 3.

α	0	10^{-4}	10^{-3}	10^{-2}	10^{-1}	ICCG
λ_{per}	0.164	0.0825	$9 \cdot 10^{-4}$	$9 \cdot 10^{-6}$	$9 \cdot 10^{-8}$	$1.6 \cdot 10^{-9}$
n	14	18	27	38	56	54

Table 3: Newly introduced small eigenvalue (λ_{per}) and number of iterations (n) needed before DICCG (or ICCG) reaches the required accuracy (perturbation α in the whole domain)

4.3 The influence of the geometry on small eigenvalues

Initially we have assumed that a high-permeability domain, which is connected to a Dirichlet boundary does not lead to a small eigenvalue. In this section this assumption is investigated in more detail.

We consider five test problems. The geometry of the problems is presented in Figure 2. All problems

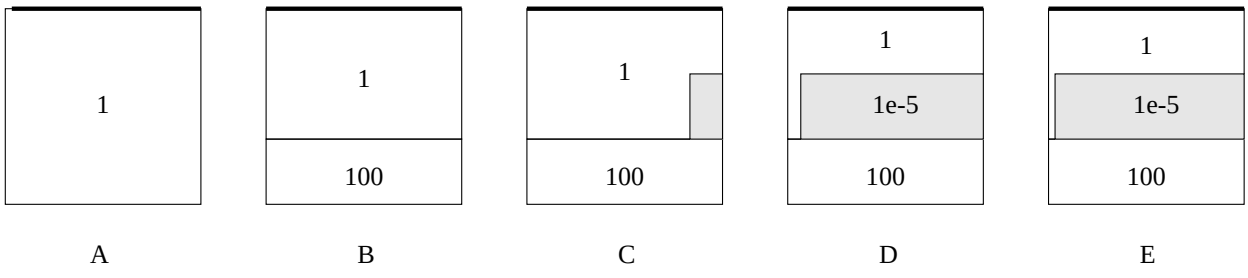

Figure 2: The test configurations with the permeability constants

are solved on an equidistant grid. The first problem is only used for reference. In the second geometry another high-permeability domain is added. In the remaining problems, the connection between both high-permeability domains is decreased due to a low-permeability layer. The smallest eigenvalue of the diagonally scaled matrices are given in Table 4. The results show clearly that adding another

configuration	A	B	C	D	E
connection width [%]	-	100	90	10	1
50×45 grid	2.7×10^{-4}	4.9×10^{-6}	4.6×10^{-6}	6.9×10^{-7}	-
100×90 grid	6.8×10^{-5}	1.2×10^{-6}	1.1×10^{-6}	1.7×10^{-7}	2.3×10^{-8}

Table 4: The smallest eigenvalues for various test problems, including variations of the connection width

high-permeability domain with no Dirichlet boundary conditions decreases the smallest eigenvalue by a factor 55. This is of the same order as the contrast in the permeability constants in both domains. On top of that the smallest eigenvalue decreases proportionally to a decrease of the connection width. Both effects enhance each other. Since the ratio between the eigenvalues of the various configurations is independent of the grid-size, we expect that the smallest eigenvalue of the continuous problem has the same behavior.

Based on these results we make the following observations:

- When a problem is considered with high, medium and low-permeability domains then a small eigenvalue occurs when a high-permeability domain is only connected to a Dirichlet boundary via a medium or a low-permeability domain.
- A high-permeability domain which is 'weakly connected' (which means that the connection width is small) to a Dirichlet boundary leads to a small eigenvalue.

These observations imply that the method to construct the projection vectors (Definition 3.2) should be refined in more general problems. In Section 5.3 a groundwater flow problem is solved, which contains high, medium, and low-permeability domains, together with 'weakly connected' high-permeability domains.

5 Numerical experiments

In this section we consider three test problems. The first problem is a three-dimensional layered problem motivated by transport of oil in a reservoir. Secondly a test problem is considered with many high-permeability inclusions in a low-permeability layer. Finally the third problem is the simulation of a two-dimensional groundwater flow.

5.1 An oil flow problem

For the flow simulation of oil and natural gas in a reservoir it is necessary to predict fluid pressures in rock layers. Therefore the diffusion equation (1) has to be solved in large three-dimensional geometries with a layered structure.

As a first problem we consider two sandstone layers ($\sigma = 10^{-4}$ and $\sigma = 10$) separated by shale layers

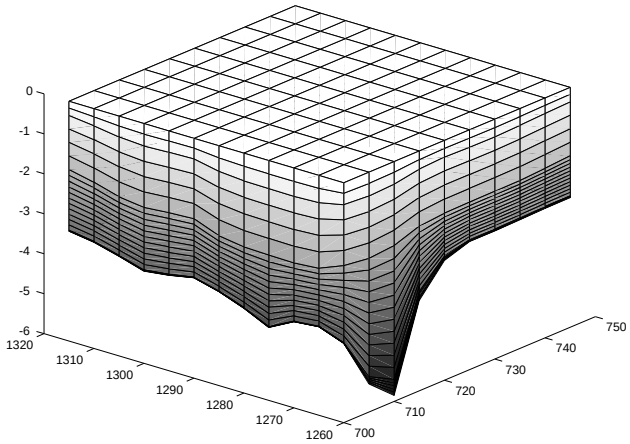

Figure 3: The geometry of an oil flow problem

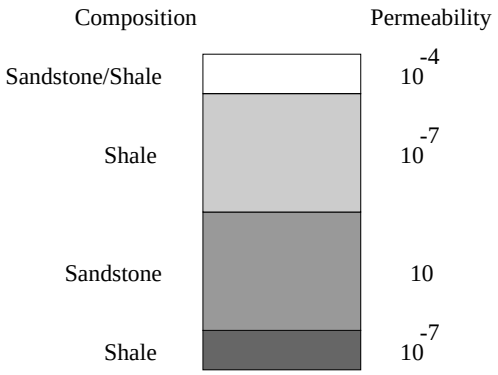

Figure 4: Permeabilities for each layer

($\sigma = 10^{-7}$). The layers vary in thickness and orientation (see Figure 3 and 4). At the top of the first sandstone layer a Dirichlet boundary condition is posed, so there is only one small eigenvalue. The number of iterations and the total CPU time for (D)ICCG are shown in Table 5 for various grid sizes. The CPU time to construct the projection vector is given too. We see that the construction time is

nodal	ICCG		DICCG		
points	iterations	CPU	iterations	CPU	CPU construction
2760	21	0.57	10	0.36	0.08
19665	38	9.01	20	5.80	0.60
148185	86	163	43	99.6	5.4

Table 5: Number of iterations and CPU time for various grid sizes

relatively small.

Next we consider the same geometry, but now the domain consists of 9 layers. Five sandstone layers are separated by 4 shale layers. The matrix of this problem has 4 small eigenvalues. Only $1.5n$ memory positions are required to store the 4 projection vectors. The (D)ICCG results are given in Table 6. There is a large gain in number of iterations and CPU time. The convergence history of both methods is shown in Figure 5 and 6. The norm of the ICCG residual has 4 bumps (corresponding to the number of small eigenvalues) before the true error decreases. In this example the second and third bump nearly coincide. The observed properties of (D)ICCG correspond well with the observations made in [16] for simple two-dimensional test problems.

For the 9 layer problem we also investigate the effect of the jump in the permeabilities. We use the grid with 19665 nodal points, take the permeability in the sandstone layers equal to 1 and vary the permeability in the shale layers. The results in Table 7 confirm that DICCG is independent of the value of σ_{shale}. In our experiments a relative high accuracy (10^{-5}) is used. In Table 8 the results are given for other accuracies. We conclude that the gain in CPU time is very large for accuracies ($10^{-1}, 10^{-2}$) which are sufficient in many applications.

nodal	ICCG		DICCG		
points	iterations	CPU	iterations	CPU	CPU construction
2760	47	1.19	10	0.37	0.12
19665	83	19.1	20	6.22	1.29
148185	189	350	44	108	12.7

Table 6: Number of iterations and CPU time for the 9 layer problem

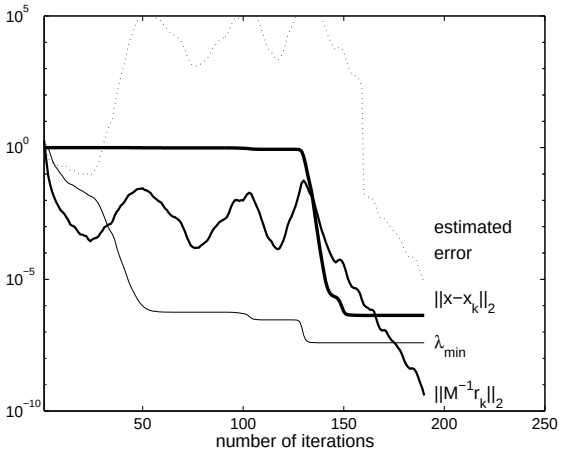

Figure 5: The convergence behavior for ICCG

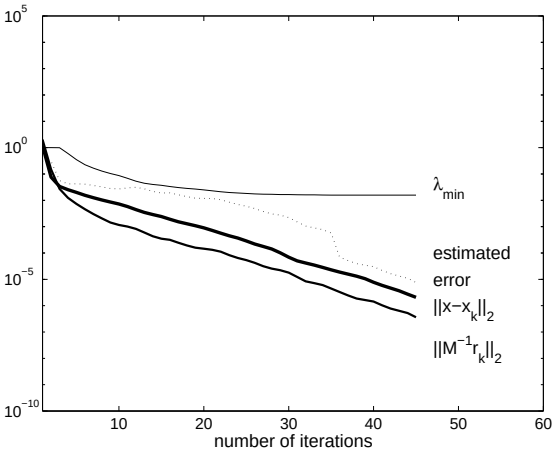

Figure 6: The convergence behavior for DICCG

σ_{shale}	ICCG		DICCG	
	λ_{min}	iterations	λ_{min}	iterations
10^{-3}	$1.5 \cdot 10^{-2}$	26	$6.9 \cdot 10^{-2}$	20
10^{-4}	$2.0 \cdot 10^{-3}$	39	$8.7 \cdot 10^{-2}$	19
10^{-5}	$2.2 \cdot 10^{-4}$	59	$7.7 \cdot 10^{-2}$	20
10^{-6}	$2.2 \cdot 10^{-5}$	73	$7.8 \cdot 10^{-2}$	20
10^{-7}	$2.3 \cdot 10^{-6}$	82	$7.7 \cdot 10^{-2}$	20

Table 7: The smallest nonzero eigenvalue and the number of iterations for the 9 layer problem

accuracy	ICCG		DICCG	
	iterations	CPU	iterations	CPU
10^{-5}	82	18.9	20	6.3
10^{-4}	80	18.4	16	5.2
10^{-3}	78	18.0	12	4.1
10^{-2}	77	17.8	3	1.5
10^{-1}	75	17.2	2	1.2

Table 8: Varying the accuracy for the 9 layer problem

5.2 A problem with many high-permeability inclusions

At the end of Section 3 we have noted that one can think of problems where the amount of memory to store the projection vectors is proportional to the number of small eigenvalues. To diminish the

required amount of memory we have proposed to use a drop tolerance (*droptol*). The components of the projection vectors which are less than *droptol* are set equal to zero. In this subsection we investigate the influence of *droptol* on the properties of DICCG.

We consider a 3 layer problem, where the shale layer contains 8 sandstone inclusions (see Figure 7). There are 12585 nodal points used in the finite element discretization of this problem. For one of the

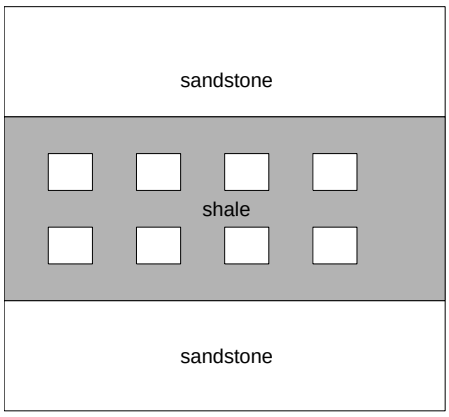

Figure 7: A problem with 8 sandstone inclusions in the shale layer

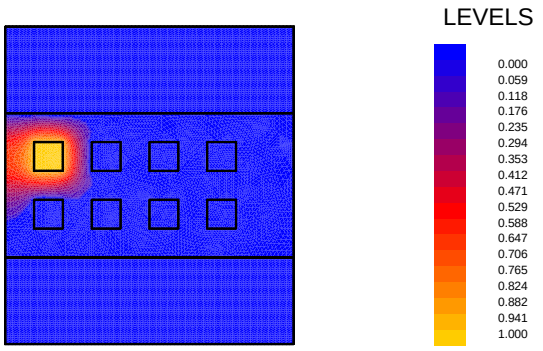

Figure 8: Contour plot of one of the projection vectors

projection vectors a contour plot is given in Figure 8. From this figure we see that the value of the projection vector is very small in the shale layer except in the vicinity of one sand inclusion. This observation has motivated us to delete the small components of the projection vectors.

In Table 9 the relevant results are given for ICCG and DICCG for various values of *droptol*. We see again a large decrease in CPU time and number of iterations when deflation (DICCG) is used. However in DICCG, $3.9n$ extra memory positions are required to store the projection vectors. Increasing the drop tolerance leads to the same number of iterations, less CPU time, a small increase in the true error, and a large decrease of the amount of extra memory. So the combination of DICCG with a drop tolerance leads to an efficient solution method even when the problem has many high-permeability inclusions.

	ICCG	DICCG		
droptol		0	10^{-2}	10^{-1}
CPU	44	12	8.3	8.1
CPU construction	0	3.1	2.9	2.9
iterations	616	76	76	76
$\lambda_{\min}$	4×10^{-9}	8×10^{-3}	8×10^{-3}	8×10^{-3}
true error	7×10^{-7}	1.86×10^{-5}	1.87×10^{-5}	2.28×10^{-5}
extra memory	0	$3.9n$	$1.6n$	$1.2n$

Table 9: Results of ICCG and DICCG for various values of *droptol*

5.3 A groundwater flow problem

In Section 4.3 we have seen that a small eigenvalue occurs when a high-permeability layer is 'weakly connected' to a Dirichlet boundary. In this section we will examine the validity of this assumption in more detail. In [15] a Poisson-like equation has been solved on the structure shown in Figure 9. The solution satisfies the equation:

$$-\nabla \cdot (A\nabla u) + B(x,y)u_x = F, \text{ where } B(x,y) = 2e^{2(x^2+y^2)}.$$

The coefficient A is defined as shown in Figure 9. The function F is everywhere zero except in the

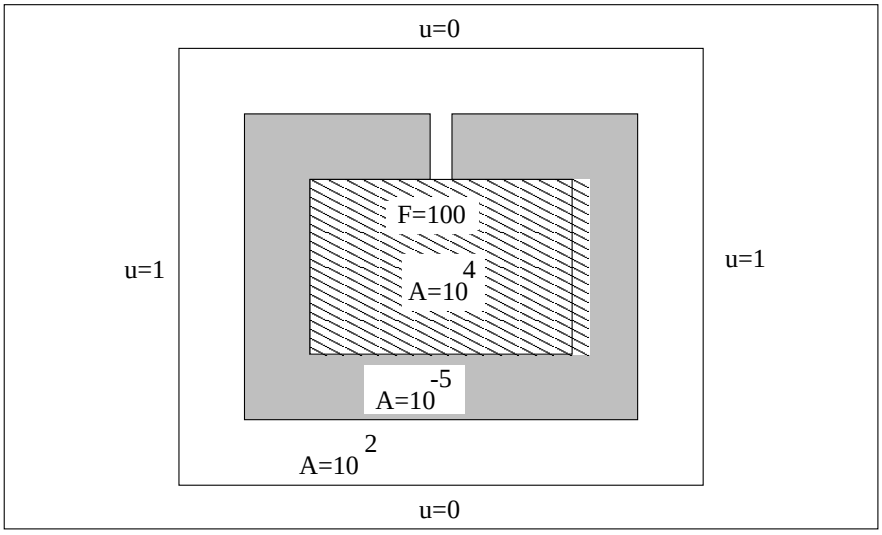

Figure 9: The coefficients and geometry of the groundwater problem

center section where $F = 100$. We have Dirichlet conditions on the complete outer boundary. In [15], BI-CGSTAB and CGS have been used to solve the discretized system. In both cases an incomplete LU-factorization has been used as preconditioner. If we take a look at the convergence behavior of BI-CGSTAB and CGS as reported in [15], there is a strong resemblance with the convergence behavior of ICCG applied to layered problems.

Since at this moment we are only interested in symmetric problems we will analyze the Poisson equation: $-\nabla \cdot (A\nabla u) = F$. Like before the smallest eigenvalue of the discretized system has been calculated. Both the presence of the clay section ($A = 10^{-5}$) as well as the jump in permeabilities between the two sand sections have an influence on the smallest eigenvalue. To annihilate the effect of the smallest eigenvalue on the convergence, DICCG has been applied to this problem. The projection vector has been constructed by neglecting the small gap in the low-permeability layer. The convergence behavior for ICCG and DICCG (applied to the original geometry) is plotted in Figure 10 and 11. The convergence behavior of DICCG is much better than that of ICCG. The number of iterations decreases with a factor two and a proper termination criterion can be used.

6 Conclusions

It has been shown that the IC preconditioned matrix is scaling invariant. This property is used to show that the number of small eigenvalues of the IC preconditioned matrix is equal to the number of high-

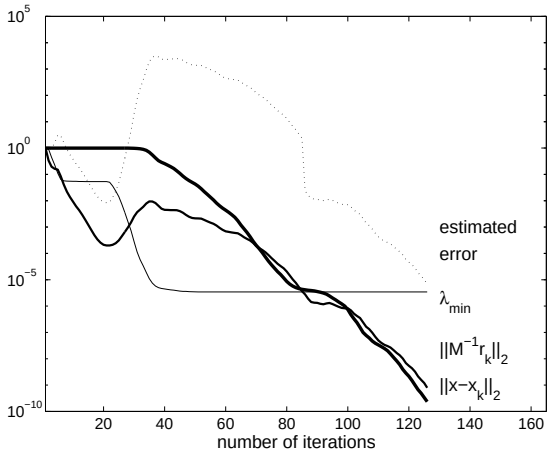

Figure 10: The convergence of ICCG

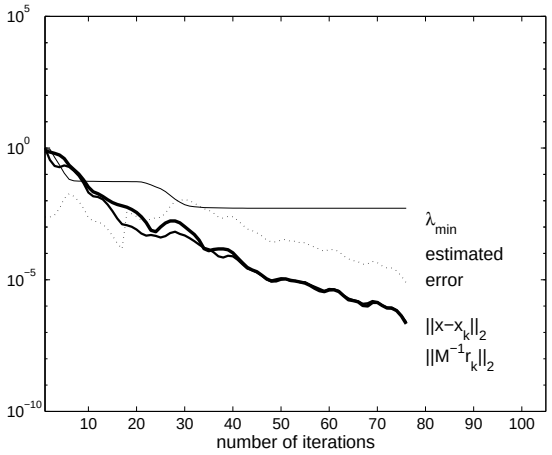

Figure 11: The convergence of DICCG

permeability domains, which are not connected to a Dirichlet boundary.

A detailed description has been given how to construct the projection vectors in a cheap way. A proof is given to show that the span of these vectors approximates the 'small' eigenspace of the diagonal or IC preconditioned matrix. This implies that the convergence behavior of DICCG is independent of the size of the jump in the coefficients.

It has been shown that perturbations of the projection vectors in the low-permeability part have only a limited influence on the convergence properties of DICCG. This has important consequences for the efficiency of the method:

- It is sufficient to compute a low-accuracy solution of the subdomain problems, which are used in the construction of the projection vectors.
- Small components of the projection vectors can be neglected to save work and memory requirements.

The use of our projection vectors in combination with the DICCG method, makes the solver robust for elliptic problems with highly discontinuous coefficients. For this kind of problems a robust stopping criterion is available, which is not the case for the standard ICCG method. For high accuracies the DICCG method converges considerably faster than the ICCG method. However, for practical accuracies the gain is enormous. This means that in the context of non-linear problems or time-dependent problems DICCG is far superior above ICCG.

It has been shown that the construction of the projection vectors can be done fully automatically and that the method can be applied to practical problems.

We conclude that DICCG with a drop tolerance is a very robust and extremely efficient method to solve problems with extreme contrasts in the coefficients.

References

[1] J. Bear. *Dynamics of fluids in porous media*. American Elsevier publishing company, New York, 1972.

[2] C.H. Bischof, J.G. Lewis, and D.J. Pierce. Incremental condition estimation for sparse matrices. *SIAM J. Matrix Anal. Appl.*, 11:644–659, 1990.

[3] X. Cai, B.F. Nielsen, and A. Tveito. An analysis of a preconditioner for the discretized pressure equation arising in reservoir simulation. *IMA J. Numer. Anal.*, 19:291–316, 1999.

[4] A.K. Cline, C.B. Moler, G.W. Stewart, and J.H. Wilkinson. An estimate for the condition number of a matrix. *SIAM J. Num. Anal.*, 16:368–375, 1979.

[5] H. De Gersem, S. Vandewalle, and K. Hameyer. A finite-element/equivalent-circuit two-level method for magnetic field simulations. In E. Dick, editor, *6th European Multigrid Conference EMG'99, Gent, Belgium, September 27-30, 1999*, pages –, Berlin, 1999. Springer.

[6] Melvyn R. Giles. *Diagenesis: a quantitative perspective; implications for basin modelling and rock property prediction*. Kluwer, Dordrecht, 1997.

[7] G.H. Golub and C.F. van Loan. *Matrix Computations third edition*. The Johns Hopkins University Press, Baltimore, 1996.

[8] I.G. Graham and M.J. Hagger. Unstructured additive Schwarz-conjugate gradient method for elliptic problems with highly discontinuous coefficients. *SIAM J. Sci. Comp.*, 20:2041–2066, 1999.

[9] E.F. Kaasschieter. A practical termination criterion for the conjugate gradient method. *BIT*, 28:308–322, 1988.

[10] E.F. Kaasschieter. Preconditioned conjugate gradients for solving singular systems. *J. Comp. Appl. Math.*, 24:265–275, 1988.

[11] G.M. Kobelkov. On the solution of the boundary value problem for the diffusion equation with highly varying coefficient. *Russian J. of Num. Anal. and Math. Model.*, 11:487–495, 1996.

[12] J.A. Meijerink and H.A. Van der Vorst. An iterative solution method for linear systems of which the coefficient matrix is a symmetric M-matrix. *Math. Comp.*, 31:148–162, 1977.

[13] B.F. Nielsen and A. Tveito. On the approximation of the solution of the pressure equation by changing the domain. *SIAM J. Appl. Math.*, 57:15–33, 1997.

[14] A. Padiy, O. Axelsson, and B. Polman. Generalized augmented matrix preconditioning approach and its application to iterative solution of ill-conditioned algebraic systems. Report 9922, KUN Mathematisch Instituut, Nijmegen, 1999.

[15] H.A. van der Vorst. Bi-CGSTAB: a fast and smoothly converging variant of Bi-CG for solution of non-symmetric linear systems. *SIAM J. Sci. Stat. Comp.*, 13:631–644, 1992.

[16] C. Vuik, A. Segal, and J.A. Meijerink. An efficient preconditioned CG method for the solution of a class of layered problems with extreme contrasts in the coefficients. *J. Comp. Phys.*, 152:385–403, 1999.